Fast Real Time 1D Barcode Detection From Webcam Images Using the Bars Detection Method

Abderrahmane NAMANE, Madjid AREZKI

***Abstract*— The detection of 1D barcode from blurry, low contrast and low resolution images is still a challenging problem. 1D barcodes are constituted by a number of bars. In this work, a new bar detection method (BDM) is developed for accurate and very fast 1D barcode detection. The least square method is introduced to determine accurately the orientation of the detected bars. Two probability density functions (PDF) of the bars length and orientation are used and applied to the detected bars in order to determine the dominant orientation and length of the existing bars. Finally, the Hough transform (HT) is applied through these detected bars centroids, in order to the bars that are next to each other, and lie on the same line support which corresponds to the barcode orientation. Excellent results were achieved on still images from two standard one-dimensional barcode datasets: WWU Muenster Barcode Database and ArTe-Lab 1D Medium Barcode Dataset. Experimental results show that our algorithm can obtain better 1D barcode detection compared with existing methods. They show that the ability of the model yield relevant and robust barcode detection even with low resolution and blurred frames, and for twisted barcodes. The proposed method shows 100% accuracy in real time applications..**

***Index Terms*—1D barcode detection, orientation estimation, least square method, Hough transform**

I. Introduction

The barcode systems have become increasingly involved in many fields of daily life. They are easy to use and make possible to enter the data much more quickly than by manual methods and are highly reliable. Their speed and reliability allow improving many operations, such as manufacturing, forwarding, reception and packing, orders preparations, inventory, and management of files. Barcodes can be found in the supermarkets, the libraries, the banks of blood, the factories…etc. They are used with reading devices in manual or automatic mode. A barcode is usually decoded using a laser device. This device exists in two types of reading modes. In the first type, the product has to be maintained in such a way that the barcode appears horizontal; it's the simplest type of barcode reader. But in the second type the barcode product can appear at any arbitrary orientations, due to a rotated mirror attached to a small motor. Barcodes can be also read using digital cameras and in real time, using image processing techniques [1][2]. This requires accurate and fast detection of the 1D barcode in order to speed up the barcode reading and can process in real time.

Most of the commercial systems like those based on laser beam or camera devices for barcode acquisition use a number of predefined angles to scan a given barcode. They usually use different orientations; 0, 22.5, 45, 67.5, 90, 112.5, 135 and 157.5° to detect a barcode. This results generally in eight orientations with a resolution of 22.5 degrees. However the reading time when using digital images, is proportional to the number of predefined orientations; this makes the system to become slower and does not suit for real time applications. The search of barcode in a product image using a camera device is not a trivial task.

In the last decade, many works focused on the detection and localisation of 1D barcode for real time reading or decoding [3][4][5]. These works could be categorized through four groups: the techniques based on morphological operations, image scanning, bottom-hat filtering, and distance transforms [6]. The 1D barcode detection is a challenging problem due to:

1-Blurry, low contrast and low resolution image barcode.
2-Execution time: it is greater than 80ms on PCs for 640x480 pixels images and for all the recent works.
3-Rotated barcodes (arbitrary orientation).

Our main idea is to track the bars in product image in order to detect the 1D barcode. In this paper we use a different approach based on filtering, binarization, outer contour detection, bars detection with BDM, LS for bars orientations, dominant bars orientation estimation (θ_d) with the first PDF, dominant bars length estimation (l_d) with the second PDF and Hough transform through only the dominant bars orientation (θ_d+90°) which makes our work accurate and very fast, and suits for real time application (Fig. 1).

Manuscript received March 20, 2017. This work was supported in part by the Algerian MESRS (Higher Studies Ministry of Scientific Research.

A. Namane is with the University Saad Dahlab of Blida, Dept. of Electronics, Signal and Image Laboratory, Route de Soumaa BP.270, Blida, Algeria (phone: 025433850; fax: 025433850; e-mail: namane_a@ yahoo.fr).

M. Arezki is with the University Saad Dahlab of Blida, Dept. of Electronics, Signal and Image Laboratory, Route de Soumaa BP.270, Blida, Algeria (phone: 025433850; fax: 025433850; e-mail: arezki_md@ yahoo.fr).

.

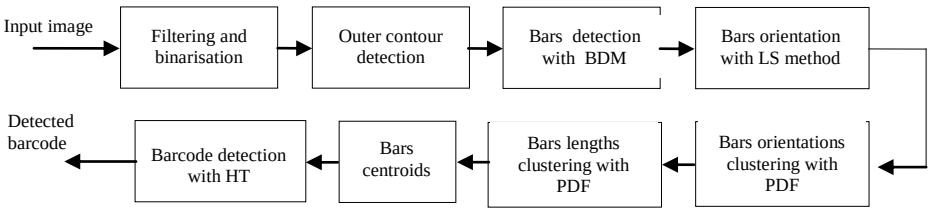

Fig. 1: Proposed method block diagram.

II. Previous work

In spite of significant improvements in the area of barcode reading, the detection and localization of barcodes in low resolution, low contrast and blurred images, is still lacking satisfactory solutions [7][8][9]. Studies on designing systems for barcode detection were in progress during the last decade [10][11][12]. Janapriya et al. [3] proposed a method for barcode recognition using webcam. The method is based, first, on the detecting and localizing the barcode. The procedure is based on a number of steps; they transformed the image input into image edges, and morphological dilation was applied through four directions (0°, 45°, 90° and 135°). Then a higher response coming from an absolute difference of two images is selected. Dilation and erosion are applied to that contour. They introduced a formula to select the blob which corresponds to barcode area from that image. Their detection method involved several low levels processing which makes the method time consuming, particularly for real time applications like those using mobile phone for image acquisition. Chai and Hock [8] used a block-based technique to locate a barcode. Their work rely on seven operations, namely, transformation of the input into non overlapping blocks of size 32 by 32 image, binarization of every block independently by using a global thresholding, skeletonization of each binarized block, connected component labeling, label region block orientation is estimated using the 2nd order moment. Their work involved the whole image pixels in the seven operations starting with non-overlapping blocks and ending with 2^{nd} order moment. This makes their method time consuming and finally not suitable for real time applications. Gallo and Manduchi [11] developed a localization algorithm assuming that the unfocused image of the barcode is captured with the camera oriented so that its vertical axis is approximately parallel to the bars. Thus, in correspondence of a barcode, one should expect an extended region characterized by strong horizontal gradients and weak vertical gradients. Accordingly, they first compute the horizontal and vertical derivatives at each pixel and then combine them together in a nonlinear fashion. Their localization can only detect barcodes that are horizontal and not in any orientation. Furthermore, they used cropped images of barcode (manually detected). Zamberletti et al. [7] presented a novel method for barcode detection in camera captured images based on a supervised machine learning algorithm that identifies one dimensional barcodes in the two-dimensional Hough Transform space. They use a properly trained supervised machine learning model that identifies the rotation angle of every barcode in real world images. The detected barcode orientation is considered correct if it differs by at most ±10° from the true rotation angle. Thus their orientation approach lacks orientation accuracy and cannot be generalized to other 1D barcode like those of Code128, code39, 2/5, which could be of length greater than six times their width. Creusot and Munawar [6] used a different approach based on detecting, filtering and clustering blobs. Most specifically, they take advantage of the detection stability of the Maximal Stable Extremal Region (MSER) system. In their work, the shape of the blobs is a strong first clue for filtering. The barcode regions are detected by clustering in a transformed feature space that uses, among other things, a representation of the perpendicular middle line to the barcode. However, their works is time consuming due to the use of MESRS which is the most computationally expensive part that takes an average of 49 ms per frame. Finally their work can process only ten frames per second. For higher Jaccard threshold accuracies (>50) the detection ability falls rapidly to zero, which means that the system lacks performances in detecting barcodes with higher accuracies.

Gabor and Flörkemeier [12], Bodnar and Nyul [5] and Wachenfeld et al. [10] use detection for nearly horizontal or vertical barcodes. Furthermore the work of Gabor and Flörkemeier [12] addresses the problem of out of focused images from mobile phones; the mobile has to be kept in vertical position. According to Creusot and Munawar [6], the only existing and relevant technique for detecting rotated 1D barcode is that of Zamberletti et al. [7]. We found according to the state of the art, that the works in [6][7] are the most relevant in detection accuracy and processing time of 1D barcode, based on still images from two standard one-dimensional barcode datasets: ArTe-Lab 1D Medium Barcode Dataset [7] and WWU Muenster Barcode Database [10].

III. Proposed method

The proposed detection method is based primarily on the eight main steps shown in Fig. 1, performed sequentially. The input image of the system represents outer contours of the captured scene. This image is obtained after preprocessing, where the filtering, binarization and contour detection are ensured by Gaussian filtering, local binarisation method [13] and border following algorithm [14] respectively.

A. Bar detection method

In this step, the bar is represented by its outer contour (Fig. 2), and its bar length *d* can be expressed as follows:

$$d = \sqrt{(x_{max} - x_{min})^2 + (y_{max} - y_{min})^2} \qquad (1)$$

ISBN: 978-988-14047-4-9
ISSN: 2078-0958 (Print); ISSN: 2078-0966 (Online)

This equation could be written theoretically in two forms based on the orientations; 0° or 45° of the bar to give d_H and d_D respectively (Fig. 2) as follows:

$$d_H = \sqrt{L^2 + l^2} = L\sqrt{1+\left(\frac{l}{L}\right)^2} \quad (2)$$

$$d_D = L + l \quad (3)$$

Equation (2) and (3) could be simplified if we assume that $l << L$, then we obtain:

$$d_H = d_D = L.$$

The bar contour length P_c of the bar must be compared to its bar length d (d_H or d_D) in order to detect the existing bars in the image using the following parameter ratio:

$$k = \frac{P_c}{d} \quad (4)$$

where $P_c = 2\,(L + l)$ (5)

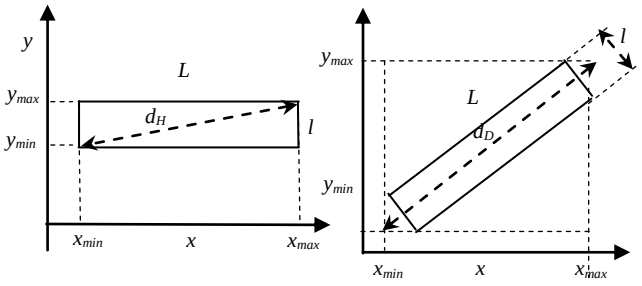

Fig. 2: Bar description.

By substitution of equation (2) and (5) into (4), and equation (3) and (5) into (4) we obtain two parameters ratio as follows:

$$k_H = \frac{2\cdot(L+l)}{L\sqrt{1+\left(\frac{l}{L}\right)^2}} \quad (6)$$

$$k_D = \frac{2\cdot(L+l)}{L+l} = 2 \quad (7)$$

Equation (6) could be simplified if we assume that $l << L$, then we obtain :

$$k_H = 2 + 2\frac{l}{L} \quad (8)$$

It can be noticed from equation (7) that all bars with orientation around 45° have their k_D always close to the value 2. This value increases gradually when going from 45° to 0° or from 45° to 90°, to converge to the ratio k_H. The value of k_H can take the value 2 for L>40l. The value of the *threshold ratio* k_{th} is determined experimentally (subsection 4.4) and equal to 2.34. Hence, from equation (4) bars can be detected using the following inequality:

$$P_c \le k_{\text{th}} \cdot d \quad (9)$$

Equation (9) is a condition which means; if the bar contour length of a given shape is less or equal to 2.34 times its bar length, then it is considered as bar, otherwise it is not, and will not be considered for orientation calculation using the LS method. There are two types of bars; thin and thick bars. In the first type of bars (Fig. 3), where $l << L$, and consequently the parameter ratio k is equal or too close to the value 2 when using equations (7) and (8). However, in the second type, the value of k for 45° of orientation with at most ±7° is always equal or too close to the value 2 according to equation (7) (Fig. 3). But for nearly horizontal or vertical bars, the value of k can take the value 2 plus an amount of $2l/L$ as mentioned earlier by equation (8).

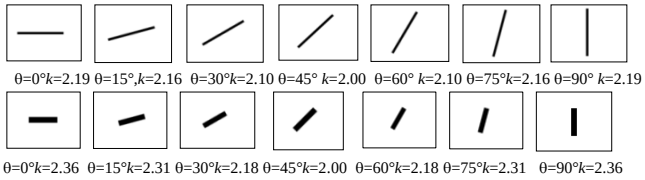

Fig. 3: Experimental results of thin and thick bars and their corresponding values of k for different orientations.

The application of the BDM which is based on the inequality (9) to an input image represented by its outer contours, tends to eliminate all the objects that are not bars as depicted in Fig. 4.

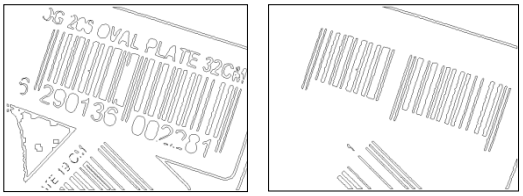

Fig. 4: Results of BDM a) Outer contour image b) Application of the BDM to the image of (a).

B. Outer contour to line transformation

The objective of this step is to extract only the two parallel lines from a detected bar as shown in Fig. 6. The bars extremities must be cut in order to get only two straight parallel lines that have exactly the same orientation as the bar. To do so, the bar length L is divided into eight equal intervals of length b, which results in four segments on both sides of the bar center (N, M) as shown in Fig. 5 (b). Figure 6 shows the detected lines after elimination of the fourth part from each side of the bar.

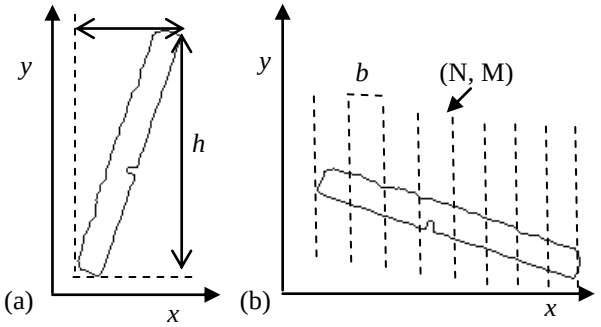

Fig. 5: x-y plan rotation and bar division (a) Bounding box bar with the height greater than the width b) Bar rotation by 90° and division into eight equal intervals.

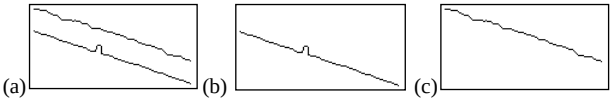

Fig. 6: Bar lines extraction a) Ends bar elimination b) Lower bar line c) Upper bar line.

ISBN: 978-988-14047-4-9
ISSN: 2078-0958 (Print); ISSN: 2078-0966 (Online)

The resulted two lines are processed separately to ad certain robustness to the orientation calculation. Each of the detected lines is first sampled into intervals or line segments of size δx of ten pixels length (Fig. 7). The center of gravity or centroid of coordinates (x_c, y_c) of each line segment is calculated using the first order moment as follow:

$$x_c = \frac{m_{10}}{m_{00}} \quad , \quad y_c = \frac{m_{01}}{m_{00}} \qquad (10)$$

where : $$m_{pq} = \sum_{x=0}^{10\text{-}1} \sum_{y=0}^{h} x^p \cdot y^q f(x,y) \qquad (11)$$

f(x,y) is the pixel intensity belonging to the line segment and equal to 1. The data entry of the least square method are then the set of ordered sequence of coordinate centroids $\{(x_0,y_0), (x_1,y_1),\ldots (x_n,y_n)\}$.

C. Least squares for bar orientation calculation

The method of least squares [15] is based primarily on the minimization of the sum of the deviations squared (*least square error*) between a given set of data and the curve that fits this set.

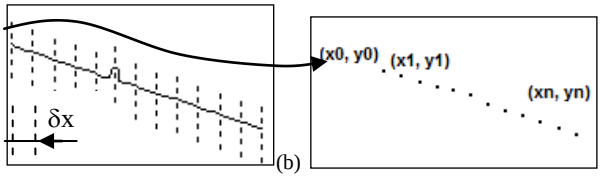

Fig. 7: Line transformation a) Sampling into line segments b) Line segments centroid determination.

Suppose that the set of data are $\{(x_0,y_0), (x_1,y_1),\ldots (x_n,y_n)\}$, where *x* is the independent variable and *y* is the dependent variable. To approximate this set of data, with $n \geq 2$, the LS method for straight line fitting uses the following equation:

$$y = a \cdot x + b \qquad (12)$$

The coefficients *a* and *b* are obtained as follows:

$$a = \frac{(n+1)\cdot c + d \cdot e}{(n+1)\cdot f - g} \quad , \quad b = \frac{e \cdot f + d \cdot c}{(n+1)\cdot f - g}$$

where: $c = \sum_{i=0}^{n} x_i \cdot y_i$, $d = \sum_{i=0}^{n} x_i$, $e = \sum_{i=0}^{n} y_i$, $f = \sum_{i=0}^{n} x_i^2$

and $g = \left(\sum_{i=0}^{n} x_i \right)^2$

The only coefficient to be calculated in this method is *a* which represents the slope of the data set (line segments) and corresponds accurately to the bar orientation:

$$\theta = \text{atan}(a) \qquad (13)$$

The only coefficient to be calculated in this method is *a* that represents the slope of the data set (sampled line) and corresponds accurately to the bar orientation. Thus, each bar from a given barcode needs two calculations to determine the orientation, one for the upper line and the other one for the lower line. By using the least square method for the 8th bar (contour) of the image in Fig. 4, we found for *lower line segment*: θ_{lo} = -18,1078 degrees and for the *upper line segment*: θ_{up} = -18,5045. The final orientation of the bar is $\theta=(\theta_{lo}+\theta_{up})/2$= -18,3061 degrees. Figure 8 shows the curve fitting of this bar given by two straight lines. In spite of the bar degradation, the orientation of lower and upper line were determined perfectly.

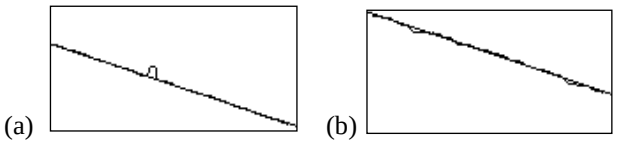

Fig. 8. Curve fitting with LS method a) Lower line fitting with straight line of slope θ_{lo} = -18,1078 degrees b) Upper line with straight line of slope θ_{up} = -18,5045 degrees.

D. Bar orientation and length estimation

Once all bars orientations are obtained, a clustering procedure can be applied to determine the dominant orientation of the bars. The orientations are grouped into clusters for different integer values of θ ranging from 0 to 179 degrees with a resolution of δθ=1degree. An accumulator *A* is used for bar orientation. Orientations should be considered as integer values; the accumulator is then incremented for a specific integer orientation θ_i when this orientation is encountered by half resolution in both sides as follows:

$$A(\theta)=A(\theta)+1 \quad \text{if } |A(\theta)-A(\theta_i)| < \delta\theta/2 \qquad (14)$$

where |*| designates absolute value. All bars orientations contribute in the construction of *A*. To find the dominant orientation, we use a probability density function (PDF) [16] for θ ranging from 0 to 179 degrees with a resolution of δθ =1degree. With the PDF attained, the correct value is found by computing the mass center of the densest interval among the interval with a given length T. The best value for the interval T is found experimentally to be equal to 4. The densest interval is noted by λ, and the mass center m_λ of the interval λ is calculated as follow:

$$m_\lambda(\theta) = \frac{\sum_{\theta \in \lambda} \theta \cdot A(\theta)}{\sum_{\theta \in \lambda} A(\theta)} \qquad (15)$$

The dominant orientation is then given by the following equation:

$$\theta_d = \underset{k=0,1,2\ldots,179}{\text{argmax}} \{ m_\lambda(\theta_k) \} \qquad (16)$$

The bar selection of a barcode is mainly based on the dominant orientation. Hence, the barcode could be detected but sometimes with other isolated branches having the same orientation as the dominant but are not belonging to the barcode. These detected branches could affect the dominant

ISBN: 978-988-14047-4-9
ISSN: 2078-0958 (Print); ISSN: 2078-0966 (Online)

orientation when using the HT on the bars centroids coordinates to determine the overall barcode orientation. For this reason a second PDF using *B* as an accumulator, is used to keep only bars that have approximately the same length. The bar selection of a barcode is mainly based on the length *l*. The bars having *l* with a tolerance of δl=12% of the length *l* are kept and the other ones are removed from the image.

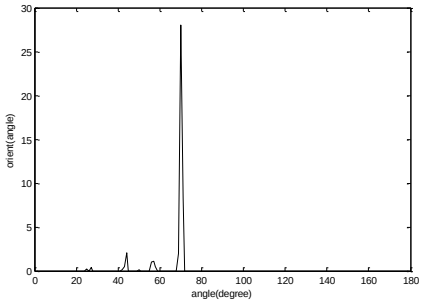

Fig. 9. PDF plot versus orientation.

IV. Experimental results

A. Dataset and bars detection

The data set represents images from WWU Muenster Barcode Database and ArTe-Lab 1D Medium Barcode Dataset. All the still images used in this experiment are of size 640x480 and constitute of 1055 and 430 samples and their corresponding ground truth images from WWU Muenster and Arte-Lab databases respectively. These images are colour, and were converted to gray levels. The binarization and border following algorithm are used to finally keep only the outer contours having less than a fixed value of pixels. This value was set experimentally to 800 pixels (length bar of 400 pixels). For each outer contour the BDM is applied to keep only objects that are considered as bars or line segments.

B. Barcode orientation

The bars orientation of a given barcode is estimated using LS method and orientation clustering as mentioned earlier. It can be noticed from figure 9 that the dominant orientation is shown by a peak around 71 degrees which corresponds exactly to the bars orientation (θ_d) of Fig. 4. Once the dominant orientation θ_d is calculated, all the bars that have their orientation less or greater than θ_d by one degree; θ_d-1$\leq\theta\leq\theta_d$+1, are kept and represented by their centroids. The O(n) of each detected bar using BDM is 2*n.

C. Metrics

To evaluate our method, it was applied to the databases, namely, the WWU Muenster and the Arte-Lab 1D databases. Our results were compared to "Robust Angle Invariant 1D Barcode Detection" (RAI-BD) method developed in [7] and "Real-time Barcode Detection in the Wild" (R-BD-W) developed in [6]. We use the same metric as in [6] [7] which is based on the Jaccard index *J* between the bounding box of the ground truth and the detection. Both the detection result *R* and the ground truth *G* are given as binary masks over the whole image [6].

$$J(R,G)=\frac{|R\cap G|}{|R\cup G|} \quad (16)$$

In this experiment we use the same evaluation parameters J_{avg} and $D_{0.5}$ as in [6]. These two metrics correspond to the average Jaccard index over the dataset and the number of images in the dataset achieving Jaccard accuracies greater or equal to 0.5 respectively. The $D_{0.5}$ corresponds to OA^{bb} in [7]:

$$D_{0.5}=\frac{\#(i\in S\,|\,J(R_i,G_i)\geq 0.5)}{|\,S\,|} \quad (17)$$

with *S* the set of files in the dataset.

Bars are detected using BDM, it's a comparison between bar contour length P_c and its bar length *d* using a threshold ratio k_{th}=2.34. This was determined experimentally based on the plot of a histogram of parameter ratio *k* (Fig. 11). The parameter ratio *k* is ranging from 1.80 to 2.60, using a calibration dataset. This
dataset represents 100 binary images of isolated barcodes, which rises to 3000 bars or line segments. To obtain these images, the input colored images of size 640x480, were preprocessed, then all the objects in these images that are not bars, were removed manually, leaving only the 30 bars of the 1D barcode per image.

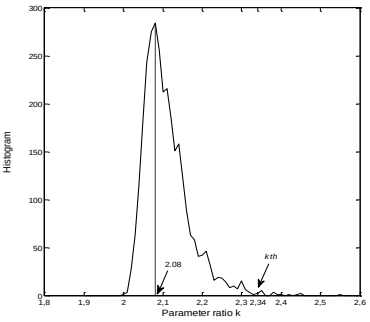

Fig. 10: Plot of histogram of parameter ratio.

From Fig. 10, it can be seen that the value of *k* for various bars, ranges from 2.00 to 2.45 and has a maximum for *k*=2.08. The value of *k* that is greater or equal than 2.35 represent bars with width *l* greater than *L*/5, which corresponds generally to very thick bars. In this experiment, we keep only values of *k* for bars width *l*<=*L*/5 which corresponds to *k*<=2.34. Furthermore, by adopting the value of k_{th}=2.34 as a *threshold ratio*, our system can detect even twisted bars and give more flexibility to bar detection method.
Plots of J_{avg} versus accuracy thresholds of the detection accuracy between our method and (Zamberletti et al., 2013; Creusot and Munawar, 2015), are given in Fig. 11, using the two datasets for varying accuracy thresholds in steps of 0.1. From these figures, it can be seen that our method outperforms clearly that of Zamberletti in low, medium and particularly high Jaccard accuracy threshold
for the two datasets. It can also show clearly that our method outperforms that of Creusot for ArTe-Lab dataset,
and for WWU Muenster for $D_{0.5}\geq$0.5. But still slightly with the same performance for $D_{0.5}$<0.5 (Muenster dataset).

ISBN: 978-988-14047-4-9
ISSN: 2078-0958 (Print); ISSN: 2078-0966 (Online)

Table 1: Comparison results using the two datasets.

Dataset	Accuracy J_{avg}			Detection Rate $D_{0.5}$		
	Zamberletti	Creusot	Ours	Zamberletti	Creusot	Ours
ArTe-Lab	0.695	0.763	**0.860**	0.805	0.893	**0.930**
WWU Muenster	0.682	0.799	**0.882**	0.829	0.963	**0.966**

Table 2: Performance improvement for Higher Jaccard accuracy thresholds.

Dataset	$D_{0.8}$ improvement (%)		$D_{0.9}$ improvement (%)	
	Zamberletti	Creusot	Zamberletti	Creusot
ArTe-Lab	52	20	330	300
WWU Muenster	129	20	847	750

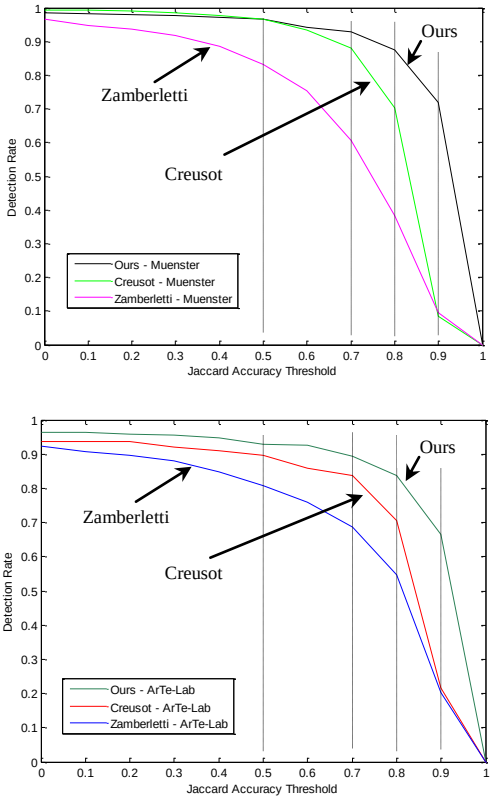

Fig. 11: Comparison of detection rates on Muenster and ArTeLab datasets.

According to Table 1, which represents comparisons results based on the accuracy rates of barcode detection; our method achieves best results and outperforms clearly the barcode detection methods [6][7]. For accuracy J_{avg}, we achieve higher accuracies; 86 and 88.2% with an improvement of 13 and 10% comparing with that of Creusot for the two datasets respectively. For a Jaccard threshold of 0.5 we succeeded in detecting the barcodes in 93% of the images for the ArTe-Lab Rotated dataset and in 96.6% for the Muenster dataset. Our method gives best performances for higher Jaccard accuracy thresholds; $D_{0.7}$, $D_{0.8}$ and $D_{0.9}$, which means that the proposed method has the ability to detect more barcodes with higher Jaccard accuracy thresholds than the two previous methods. Table 2 summarizes the high improvement of the detect accuracy for Jaccard threshold accuracies ($\geq$0.8) using our method.

Fig. 12: Sample image for Barcode detection with our method ($J(R,G)$=0.960) (left image) and result of barcode detection with Creusot (in green) and Zamberletti (in red) (right image)..

Fig.ure 13: Examples of the detection of blurry and twisted barcodes with $J(R,G)$=0.933 (left image) and $J(R,G)$=0.852 right image).

Figure 12 shows correctly detected barcode and their corresponding detection rate (left column) and those performed by Creusot (in green) and Zamberletti (in red). In spite of the low quality of the barcodes, our developed system was able to accomplish the detection with high accuracy. Figure 13 shows detection of blurry and twisted images with higher accuracies ($J(R,G)$=0.933 and $J(R,G)$=0.852) using our proposed method. Our approach achieves 1D barcode detection in 21 ms average time with

ISBN: 978-988-14047-4-9
ISSN: 2078-0958 (Print); ISSN: 2078-0966 (Online)

higher accuracy for both datasets, running on PC Intel(R) Core(TM) 2 Duo CPU E7300 @ 2.66GHz. Both works in (Zamberletti et al., 2013; Creusot and Munawar, 2015) were running on Dell XPS 9100 single core 3.34 GHz machine according to experimental results in (Creusot and Munawar, 2015). We achieve lower average processing time per frame than their methods (Table 3). All the steps that constitute our method were processed sequentially, so our machine was executing only one task at a time.

Table 3: Average computer time in millisecond.

Dataset	Zamberletti	Creusot	Ours
ArTe-Lab	**135**	105	21
Muenster	**130**	115	21

V. Conclusion

We have presented a 1D barcode detection method applied to images from two databases and to images from Webcam device. Our proposed method and system not only can detect barcodes in complex scene but also it can detect blurred barcodes due to unfocused Webcam. Our system can work in real time due to its high speed, and can process an image in 21ms. Experiments were conducted on real images of products, with a low resolution and a poor focus of the Webcam. We report experimental results that show a high achievement on two databases, namely, WWU Muenster and Arte-Lab 1D barcode, comparing with the existing methods. These results show the robustness of the proposed method. We show also that the BDM is thickness dependent, the more the bar is thin and the more its detection is evident. The proposed method shows 100% accuracy in real time applications.

References

[1] Jain, A. K., Chen, Y. "Bar code localization using texture analysis", Proceeding of the Second International Conference on Document Analysis and Recognition, pp.41-44, October 1993.

[2] H. Wakaumi, "A high-density ternary barcode detection system with a fixed period delay method," Proc. Eurosensor XXIV Procedia Engineering 5 pp. 252-255, Linz, Austria, September 2010.

[3] Ruwan Janapriya, Lasantha Kularatne, Kosala Pannipitiya, Anuruddha Gamakumara and Chathura de Silva,"A Low Cost Barcode Reader using a Web-cam," *Engineering Research Unit (ERU) Symposium*, Sri Lanka, 2003.

[4] James Juett, X. Q., "Barcode localization using bottom-hat filter", *NSF Research Experience for Undergraduates*. 2005.

[5] Bodnar P. and Nyul, L. G., "A novel method for barcode localization in image domain". In M. Kamel and A. Campilho, editors, *Image Analysis and Recognition of Lecture Notes in Computer Science*, 7950: 189-196, 2013.

[6] Creusot, C. and Munawar, A., "Real-time Barcode Detection in the Wild," *IEEE Winter on Applications of Computer Vision Conference*, 2015.

[7] Zamberletti, A., Gallo, I. and Albertini, S., 2013. Robust angle invariant 1d barcode detection. *Pattern Recognition (ACPR), 2nd IAPR Asian Conference on*, 160– 164.

[8] D. Chai,F. Hock, "Locating and decoding EAN-13 barcodes from images captured by digital cameras*," IEEE International Conference on Information, Communications and Signal Processing, IEEE Proc.* , pp 1556-1560, Thailand, Bangkok, December 2005.

[9] K. Wang, Y. Zhou, H. Wang,"1D barcode reading on camera phones," International Journal of Image and Graphics, 7(3) pp. 529-550, 2007.

[10] S. Wachenfeld, S. Terlunen, X. Jiang"Robust recognition of 1-D barcode using camera phones," *Proc. of 19th International Conference on Pattern Recognition (ICPR 2008)*, 2008.

[11] O. Gallo and R. Manduchi, "Reading 1D Barcodes with Mobile Phones Using Deformable Templates," IEEE Transaction on Pattern Analysis and Machine Intelligence, vol. 33, no. 9, pp. 1834-1843, 2011.

[12] Gabor, S. and Flörkemeier C., "Blur-resistant joint 1D and 2D barcode localization for smartphones", *In Proceedings of the 12th International Conference on Mobile and Ubiquitous Multimedia*, 2013.

[13] W. Niblack, "An introduction to digital image processing," 115-116, Englewood Cliffs, N.J.: Prentice Hall, 1986.

[14] A. Chottera and M. Shridhar, "Feature extraction of manufactured parts in the presence of spurious surface reflections," Canadian Electron. Journal, vol. 7, no. 4, pp. 29-33, 1982.

[15] Chatterjee, S., Hadi, A. and Price, B., 2000. Simple linear regression. *Ch.2 in Regression Analysis by Example*, New York, 3rd edition, Wiley, 21-50.

[16] Qi, J., Shi, Z., Ahao X. and Wang, Y., 2004. A novel fingerprint matching method based on the Hough transform without quantization of the Hough space. *Proceeding of the Third International Conference on Image and Graphics (ICIG04)*, 262-265.

ISBN: 978-988-14047-4-9
ISSN: 2078-0958 (Print); ISSN: 2078-0966 (Online)